



Experimental verification of dynamic behavior for multi-link press mechanism with 2D revolute joint considering dry friction clearances and lubricated clearances

Xiulong Chen · Shun Gao · Tao Wang

Received: 28 December 2021 / Accepted: 21 April 2022 / Published online: 13 May 2022
© The Author(s), under exclusive licence to Springer Nature B.V. 2022

Abstract The existence of clearance joints seriously affect the kinematic accuracy and service life of precision mechanisms. So as to ensure the kinematic accuracy reliability of mechanism, it is imperative to accurately predict the dynamic behavior of precision mechanism considering clearances. At present, the studies often focus on theoretical analysis and simulation verification of mechanism with clearances, while the studies verified by experiment are relatively few and often focus on simple mechanism. Moreover, most of studies centered on simple mechanism with dry friction clearance, while the studies on complex mechanism with multiple lubricated clearances are less. In this paper, the impact of multiple clearances on dynamic behavior of 2-DOF 9-bar precision press mechanism is analyzed. Firstly, the mathematical models of dry friction clearance and lubricated clearance are established and embedded into the Lagrange dynamic equation, respectively. Then, the impact of clearance values, the material of clearance-shaft and crank driving speeds on dynamic behavior of mechanism are researched. Finally, the simplified experimental platform of 2-DOF 9-bar press mechanism considering 2D revolute joint clearances is established, and the correctness of the theoretical

model is proved by experimental verification. This study not only offers theoretical guidance for the layout and life prediction of multi-link press mechanism, but also provides reference for the dynamic behavior analysis and prediction of other mechanisms.

Keywords Dry friction clearances · Lubricated clearances · Dynamic behavior · Experimental verification

1 Introduction

The multi-link press mechanisms remain more widely used because of its simple structure, easy manufacturing and control. However, due to the effects of machining accuracy, installation errors and other factors, clearance will unavoidably appear in rotating pair of mechanism. The clearance would aggravate the friction and wear between the elements of rotating pair, and seriously affect the motion accuracy and service life of mechanism [1–3]. In practical engineering, lubricant oil is usually added at the clearance joint to reduce the impact of the collision of elements between the clearance on the output of mechanisms, and thus to increase the stability and reliability [4–6]. Therefore, so as to accurately predict the effect of dry friction clearances and lubricated clearances on dynamic behavior of mechanism, to construct a

X. Chen (✉) · S. Gao · T. Wang
College of Mechanical and Electronic Engineering,
Shandong University of Science and Technology,
Qingdao 266590, China
e-mail: cxldy99@163.com

reasonable dynamic model and carry out experimental study is very meaningful.

In recent time, many scholars have studied the revolute clearance joint of mechanism. However, most of them often focus on the results of theoretical simulation and experimental research on simple mechanism with 2D revolute clearance joint, such as crank-slider mechanism and four-bar mechanism, while there are few literatures on the study of complex mechanisms considering 3D revolute clearances. Reis et al. [7] explored a new hydrodynamic lubricated model and found that this model has faster calculation speed than the traditional HD model through numerical simulation. Abdallah et al. [8] simulated dynamic behavior of flexible crank-slider system considering clearance based on ADAMS software and found that multiple clearance joints have greatly effects on system. Miao et al. [9] built the mathematical model of locking mechanism and studied the influence of clearance on its kinematic accuracy. The simulation results found that clearances have distinct effects on dynamic under different working states. Marques et al. [10] presented a model of spatial four-bar mechanism considering spherical clearance, analyzed the effects of different parameters on its dynamic behavior. Chen et al. [11] conducted experimental research on mechanism with clearances and considered the influence of factors such as dynamic viscosity on dynamic behavior of system. However, this research mainly discussed the system with lubrication clearances, and did not conduct experimental study on system considering dry friction clearances. In addition, this study did not consider the impact of the material of clearance-shaft on dynamics of system. Geng et al. [12] studied the time-varying reliability of the motion of mechanism with clearance, and quantified the uncertain impact of parameters on motion performance of mechanism. Jiang et al. [13] researched the impact of non-uniform wear clearances on dynamic response of multi-link mechanism, compared and verified the correctness of the model based on MATLAB software and ADAMS simulation software, but the article lacks the experimental verification link. Brogliato [14] performed the feedback control of system considering clearances from the aspects of collision control and trajectory tracking. Pandey et al. [15] explored the motion accuracy of robot considering clearance according to maximum entropy rule to keep its motion error within a certain range. Xiang et al. [16] proposed a hybrid

friction model to discuss the dynamic behavior of the system with clearances, and verified the rationality of this model through the motion simulation of space manipulator. Singh et al. [17] discussed the governing equation of lubricating oil flow in lubricated clearance according to finite element method, and researched the impact of non-Newtonian lubricant on bearing wear characteristic. Bai et al. [18] set up a model of three-dimensional revolute clearance and researched the effect of revolute clearances on satellite antenna system dynamics through simulation. Especially the sticking modes induced by Coulomb friction are taken into account in the framework of the paper. Erkaya [19] et al. studied the impact of joint clearance on vibration and noise characteristics of mechanism, and built a test platform of crank-slider mechanism considering clearance. The vibration and noise of system were measured by accelerometer and microphone and evaluated the vibration and noise characteristics of the mechanism with and without clearance. Flores [20] et al. built an experimental platform of crank-slider mechanism with revolute clearance joint to verify the prediction ability of multi-body clearance joint model. The correlation between numerical results and experimental results is given and discussed in this paper. Erkaya [21] et al. analyzed the influence of joint clearance on partial compliance and traditional articulated mechanism through numerical and experimental research. The influence of joint clearance on vibration of mechanism is measured by installing accelerometers at different positions. In addition, a few scholars have carried out research on mechanism system considering 3D revolute clearance joint. Akhadkar [22] et al. used non-smooth set-valued contact models and the time-stepping Moreau-Jean algorithm to perform numerical simulations for 3D revolute joints with clearances, and verified the correctness of the model by experiments. Qian et al. [23] carried out the 3D model of translational clearance joints, and used this model to discuss the nonlinear dynamic behavior of crank-slider mechanism. Federico et al. [24] conducted a novel model of 3D revolute clearance, and the effectiveness of this method was proved by numerical calculation. Wu et al. [25] presented a contact force model of 3D moving clearance and applied it to double crank mechanism and found that the moving clearance has a great impact on dynamics of mechanism.

At same time, the studies on dynamic behavior of mechanisms mostly centered on the simple mechanism considering single clearance, while the studies on complex mechanism considering multiple lubricated clearances are rare. Tan et al. [26] put forward a calculation method for solving the dynamic of spatial flexible mechanical considering spherical clearance joints according to ANCF method, and checked the method with crank-slider mechanism. Ahmedalbashir et al. [27] established a dynamic modeling and built the test platform of four-bar mechanism considering single clearance, then compared the simulation results and theoretical results, so as to verify the rationality of the established model. Wang et al. [28] carried out a novel non-penetration method of revolute clearance and verified it by crank-slider mechanism. Guo et al. [29] researched the effect of clearance between the piston and cylinder of the crank train on secondary movement. The results show that the impact of clearance on system dynamics is linked to impact response of secondary movement of the piston. Amiri et al. [30] investigated the effect of clearance joint on dynamics of crank-slider mechanism, and utilized tuned mass damper to suppress error of dynamic response. Ordiz et al. [31] proposed a useful way to discuss the impact of clearances on operation life of mechanism according to commercial software, and applied it to serial robot. Farahan et al. [32] analyzed the dynamic behavior and nonlinear characteristics of simple mechanism considering clearance based on Poincaré portraits. Zheng et al. [33] compared and studied the impact of different friction model on numerical analysis of dynamic behavior of crank-slider mechanism with clearance. Li et al. [34] considered the effect of parameter uncertainty on dynamic performance and kinematic precision of planar space deployable mechanism considering clearance. Zheng et al. [35] put forward a model of planar mechanism with clearance considering viscosity, and took crank-slider mechanism as an example to prove that viscosity will infect the dynamic characteristics of system.

To sum up, previous studies often focused on dynamic simulation research of mechanism and the experimental study of simple mechanism with clearance, while there are few studies on dynamic behavior and experimental study of complex mechanisms with multiple lubricated clearances. Based on this background, this paper takes 2-DOF 9-bar press

mechanism as a research object, the dynamic behavior and experimental study of complex mechanism considering multiple clearances is researched. The arrangement of this study is as follows: In chapter 2, the mathematical models of dry friction clearance and lubricated clearance is established, respectively. In chapter 3, the dynamic model of mechanism considering clearances according to Lagrange multiplier method is developed. In chapter 4, the effects of clearance values, material of clearance-shaft and crank driving speeds on dynamic behavior of press mechanism considering dry friction clearances and lubricated clearances are analyzed and predicted. In chapter 5, a simplified experimental platform of 2-DOF 9-bar press mechanism was built, and the impact of different parameters on dynamics of platform is researched. The comparison between experimental results and theoretical results verified the correctness of the theoretical model.

2 Modeling of revolute clearance

2.1 Dry friction clearance model

In this paper, the “contact-separation-collision” three state model is used to describe the relative relationship between the elements of the revolute clearance joint [36]. The model comprehensively considers the contact, separation and collision of the elements of the revolute clearance joint in the process of motion, as well as the transition process from the collision state to the continuous contact state, which is more in line with the actual motion of the elements of the revolute clearance joint. Therefore, it is widely used in the clearance modeling of mechanisms considering revolute clearance joint, as shown in Fig. 1.

As depicted in Fig. 2, the eccentricity vector of dry friction clearance is given by

$$e_1 = r_i^P - r_j^P \quad (1)$$

where r_i^P and r_j^P represent position vectors of centroid of bearing and shaft.

Embedding depth of dry friction clearance expresses as

$$\delta = e_1 - r \quad (2)$$

where r means clearance value, and $r = R_i - R_j$.

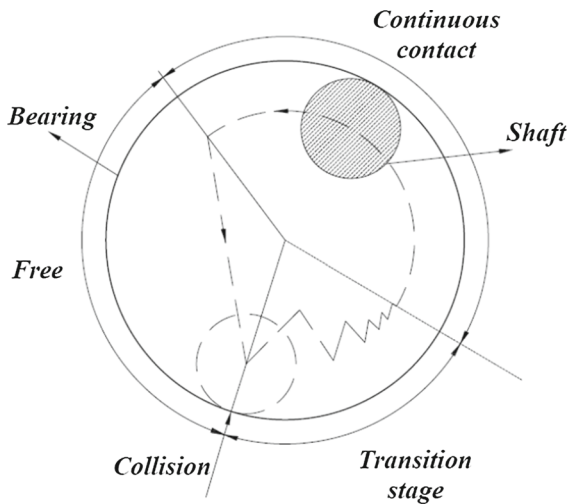


Fig. 1 Three state model of revolute clearance joint

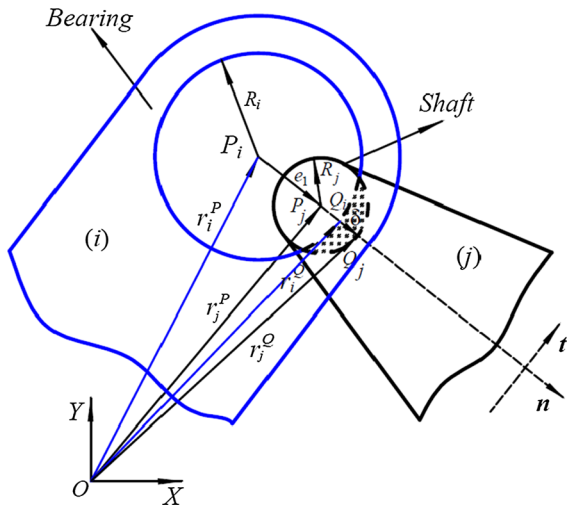


Fig. 2 Dry friction clearance model

The velocity of the collision point is decomposed into normal velocity (v_n) and tangential velocity (v_t), yielding

$$\begin{cases} v_n = (\dot{r}_i^{Q_i} - \dot{r}_j^{Q_j})^T \mathbf{n} \\ v_t = (\dot{r}_i^{Q_i} - \dot{r}_j^{Q_j})^T \mathbf{t} \end{cases} \quad (3)$$

where $\dot{r}_i^{Q_i}$ and $\dot{r}_j^{Q_j}$ represent velocity vectors at point of impact of shaft and bearing, respectively, when collision occurs.

When the mechanism is simulated, the motion state of the shaft in the bearing can be judged by the following formula

$$\begin{cases} \delta(t_n)\delta(t_{n+1}) < 0 & \text{Free state} \\ \delta(t_n)\delta(t_{n+1}) = 0 & \text{Continuous contact state} \\ \delta(t_n)\delta(t_{n+1}) > 0 & \text{Collision state} \end{cases} \quad (4)$$

where $\delta(t_n)$ represents the collision depth at the time t_n , $\delta(t_{n+1})$ represents the collision depth at the time t_{n+1} .

The Lankarani-Nikravesh (L-N) model is widely utilized to settle the normal collision force of revolute clearance [9, 32, 33], which could be expressed as

$$F_n = \frac{4\delta^n}{3(\sigma_i + \sigma_j)} \left(\frac{R_i R_j}{R_i + R_j} \right)^{\frac{1}{2}} \left[1 + \frac{3(1 - c_e^2)\delta^{\dot{\delta}^{(-)}}}{4\dot{\delta}^{(-)}} \right] \quad (5)$$

where $\sigma_m = \frac{1 - \nu_m^2}{E_m}$ ($m = i, j$), ν_m represents Poisson's ratio, E_m represents elastic modulus, $\dot{\delta}^{(-)}$ means initial impact velocity, n is exponent and set to 1.5 [20, 30], c_e means recovery coefficient.

Modified Coulomb friction model is usually utilized to settle tangential friction of clearance [11, 32], which is given by

$$F_t = -c_f c_d F_n \frac{v_t}{|v_t|} = \begin{cases} 0 & |v_t| \leq v_0 \\ -c_f \frac{|v_t| - v_0}{v_1 - v_0} F_n \text{sign}(v_t) & v_0 \leq |v_t| \leq v_1 \\ -c_f F_n \text{sign}(v_t) & |v_t| > v_1 \end{cases} \quad (6)$$

where c_f represents friction coefficient, c_d represents correction coefficient, v_0 and v_1 are the limit speed.

To sum up, the impact force of dry friction clearance can be given as

$$F_{\text{dry}} = F_n \mathbf{n} + F_t \mathbf{t} \quad (7)$$

2.2 Lubricated clearance model

Adding lubricant to the clearance is one of the most effective method to increase the stability of mechanical system, so to establish a reasonable model to describe lubricated clearance is completely necessary.

In this paper, the lubricated clearance model is built, as depicted in Fig. 3, the eccentricity vector of lubricated clearance is given by

$$e_2 = \mathbf{r}_i^S - \mathbf{r}_j^S \quad (8)$$

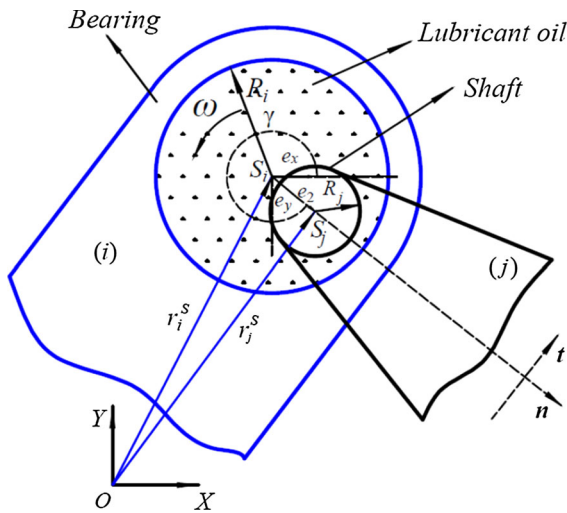


Fig. 3 Lubricated clearance model

where r_i^s and r_j^s are position vectors of centroid of shaft and bearing of lubricated clearance.

At present, Reynolds equation is usually used to solve the oil film pressure of lubricated clearance [6, 23], which could be expressed as

$$\frac{\partial}{\partial x} \left(\frac{h^3}{\mu} \frac{\partial p}{\partial x} \right) + \frac{\partial}{\partial z} \left(\frac{h^3}{\mu} \frac{\partial p}{\partial z} \right) = 6U \frac{\partial h}{\partial x} + 12 \frac{dh}{dt} \quad (9)$$

where h means film thickness, p means pressure, x and z mean radial and axial directions, respectively, μ means dynamic viscosity, U means relative tangential velocity.

The right two terms of Eq. (11) are represented wedge-film force and squeeze-film force, respectively. Because Eq. (11) is a non-homogeneous equation, so it is difficult to solve directly. In this paper, because the length to radius ratio of the bearing is larger than 2, so it can be regarded as an infinite short bearing, that is, assuming that the second term on the left of Eq. (11) is 0.

Pinkus and Sternlicht proposed a force model of lubricated clearance, when $\dot{\varepsilon} \geq 0$, the model is expressed as

$$F_{\mu r} = \frac{-6\mu R_j^3 L}{r^2} \frac{\dot{\varepsilon}}{(1 - \varepsilon^2)^{1.5}} \left(\frac{4k\varepsilon^2}{(2 + \varepsilon^2)} + \pi \frac{k + 3}{k + 1.5} \right) \quad (10)$$

$$F_{\mu t} = \frac{6\mu R_j^3 L}{r^2} \frac{\pi\varepsilon(\omega - 2\dot{\gamma})}{(2 + \varepsilon^2)(1 - \varepsilon^2)^{0.5}} \frac{k + 3}{k + 1.5} \quad (11)$$

When $\dot{\varepsilon} < 0$, the model is expressed as

$$F_{\mu r} = \frac{-6\mu R_i^3 L}{r^2} \frac{\dot{\varepsilon}}{(1 - \varepsilon^2)^{1.5}} \left(\frac{4k\varepsilon^2}{(2 + \varepsilon^2)} - \pi \frac{k}{k + 1.5} \right) \quad (12)$$

$$F_{\mu t} = \frac{6\mu R_i^3 L}{r^2} \frac{\pi\varepsilon(\omega - 2\dot{\gamma})}{(2 + \varepsilon^2)(1 - \varepsilon^2)^{0.5}} \frac{k}{k + 1.5} \quad (13)$$

In Eq. 12 to Eq. 15, ε and γ represent eccentricity ratio and offset angle, respectively. $\dot{\varepsilon}$ and $\dot{\gamma}$ represent the first derivative against time of eccentricity ratio and offset angle, respectively. And the calculation formula for each parameter is as follows: $\varepsilon = \frac{e_2}{r}$, $\gamma = \arctan \left(\frac{e_y}{e_x} \right)$, $\dot{\varepsilon} = \frac{\dot{e}_2}{r}$, $\dot{\gamma} = \frac{e_x \dot{e}_y - \dot{e}_x e_y}{e_2^2}$. Parameter k is given by $k = \left((1 - \varepsilon^2) \left(\frac{\omega - 2\dot{\gamma}}{2\dot{\varepsilon}} \right)^2 + \frac{1}{\varepsilon^2} \right)^{0.5}$, where ω means relative angular velocity.

The lubricated force would change suddenly when $\dot{\gamma}$ tends to 0. Therefore, the correction factor m is introduced to modify the model, and the modified model is given as

$$F_{mn} = \begin{cases} F_{\mu r} & \text{if } \varepsilon_0 < \varepsilon < 1 \\ \varepsilon^m F_{\mu r} & \text{if } 0 < \varepsilon < \varepsilon_0 \end{cases} \quad (14)$$

$$F_{mt} = \begin{cases} F_{\mu t} & \text{if } \varepsilon_0 < \varepsilon < 1 \\ \varepsilon^m F_{\mu t} & \text{if } 0 < \varepsilon < \varepsilon_0 \end{cases} \quad (15)$$

where ε_0 means parameter of modified interval.

Therefore, the modified lubricated force model is given as

$$F_u = \begin{bmatrix} F_x \\ F_y \end{bmatrix} = \begin{bmatrix} F_{mn} \cos \gamma - F_{mt} \sin \gamma \\ F_{mn} \sin \gamma + F_{mt} \cos \gamma \end{bmatrix} \quad (16)$$

Flores [37] presented a transition model from dry friction clearance to lubricated clearance, which solves the problem of numerical integration instability when the eccentricity is close to 1, the transition model expresses as

$$F = \begin{cases} F_u & \text{if } e_2 < r \\ \frac{(r + e_0) - e_2}{e_0} F_u + \frac{e_2 - r}{e_0} F_{Dry} & \text{if } r \leq e_2 \leq r + e_0 \\ F_{Dry} & \text{if } e_2 > r + e_0 \end{cases} \quad (17)$$

where F is the force between bearing and shaft, e_0 is offset distance.

3 Dynamic modeling of press mechanism considering clearances

The structure of 2-DOF 9-bar press mechanism is shown in Fig. 4. This mechanism includes frame (L_5), cranks (L_1, L_4), connecting rods (L_2, L_3, L_6, L_7, L_8) and slider (S_9). The slider is connected with the frame through a moving pair, and the other joints are connected by rotating pair, in which joint A and joint B are clearance joints. This mechanism has 8 movable members and 11 low pairs, so according to the DOF calculation formula, the mechanism has 2 DOF. Therefore, in order to ensure a definite movement of the mechanism, the cranks (L_1, L_4) are directly driven by the motor.

In this paper, the Lagrange multiplier method is used to model the dynamics of system, and the generalized coordinates of each member is given by

$$q_i = (x_i \ y_i \ \theta_i)^T \quad (i = 1, \dots, 9, i \neq 5) \tag{18}$$

where x_i and y_i mean generalized coordinates of member i in X and Y directions, respectively. And θ_i represents rotation angle of member i in X direction.

When considering the clearance between joints A and B, the displacement constraint equation of mechanism is given as

$$\Phi(q, t) = \begin{pmatrix} x_1 - L_{s1} \cos \theta_1; y_1 - L_{s1} \sin \theta_1; x_4 - L_{s4} \cos \theta_4; y_4 - L_{s4} \sin \theta_4 + l_5; \\ x_7 - L_{s7} \cos \theta_7 - x_2 - L_{s2} \cos \theta_2; y_7 - L_{s7} \sin \theta_7 - y_2 - L_{s2} \sin \theta_2 \\ x_7 - L_{s7} \cos \theta_7 - x_3 - L_{s3} \cos \theta_3; y_7 - L_{s7} \sin \theta_7 - y_3 - L_{s3} \sin \theta_3; \\ x_7 + L_{s7} \cos \theta_7 - x_8 + L_{s8} \cos \theta_8; y_7 + L_{s7} \sin \theta_7 - y_8 + L_{s8} \sin \theta_8; \\ x_7 + L_{s7} \cos \theta_7 - x_6 - L_{s6} \cos \theta_6; y_7 + L_{s7} \sin \theta_7 - y_6 - L_{s6} \sin \theta_6; \\ x_6 - L_{s6} \cos \theta_6 - h_x; y_6 - L_{s6} \sin \theta_6 - h_y; x_9 - L_{s8} \cos \theta_8 - x_8; \\ y_9 - L_{s8} \sin \theta_8 - y_8; x_9 - h_x; \theta_9 - 90^\circ; \theta_1 - \omega_1 t + 39.52^\circ; \theta_4 - \omega_4 t - 199.47^\circ \end{pmatrix} = \mathbf{0} \tag{19}$$

Velocity constraint equation is given as

$$\Phi_q \dot{q} = -\Phi_t \equiv v \tag{20}$$

where Φ_q represents Jacobian matrix, $\Phi_q = \frac{\partial \Phi}{\partial q}$, $\Phi_t = \frac{\partial \Phi}{\partial t} \dot{q}$ represents generalized velocity vector.

Acceleration constraint equation is acquired by first derivative of Eq. (22) against time, which expresses as

$$\Phi_q \ddot{q} = -(\Phi_q \dot{q})_q \dot{q} - 2\Phi_{qt} \dot{q} - \Phi_{tt} \equiv \gamma \tag{21}$$

where \ddot{q} represents generalized acceleration vector, $\Phi_{qt} = \mathbf{0}_{20 \times 24}$, $\Phi_{tt} = \mathbf{0}_{20 \times 1}$.

Establish the dynamic equation about Lagrange multiplier λ , which expresses as

$$M\ddot{q} + \Phi_q^T \lambda = g \tag{22}$$

where g means generalized force, M means mass matrix.

Simultaneous Eqs. (23) and (24), the dynamic equation is given as

$$\begin{pmatrix} M & \Phi_q^T \\ \Phi_q & \mathbf{0} \end{pmatrix} \begin{pmatrix} \ddot{q} \\ \lambda \end{pmatrix} = \begin{pmatrix} g \\ \gamma \end{pmatrix} \tag{23}$$

In order to acquire more stable simulation results, the Baumgarte coefficients are introduced, and the modified dynamic equation is given by

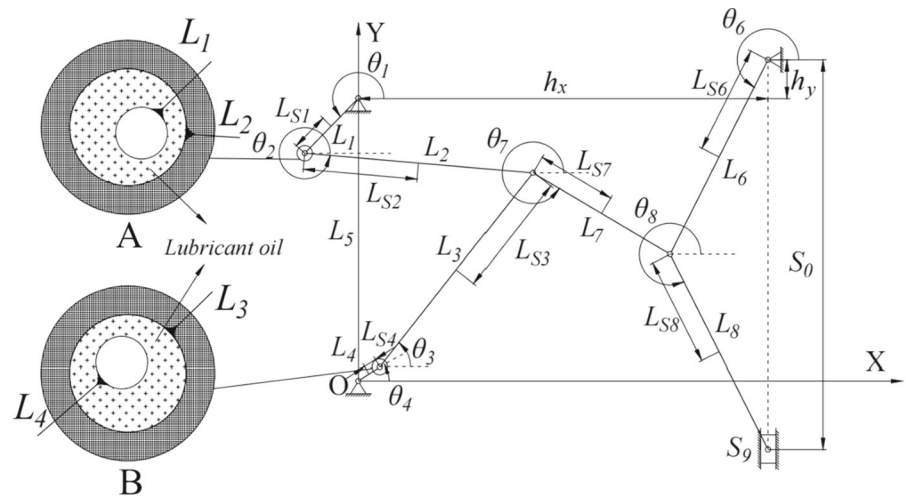
$$\begin{pmatrix} M & \Phi_q^T \\ \Phi_q & \mathbf{0} \end{pmatrix} \begin{pmatrix} \ddot{q} \\ \lambda \end{pmatrix} = \begin{pmatrix} g \\ \gamma - 2\alpha\dot{\Phi} - \beta^2\Phi \end{pmatrix} \tag{24}$$

where $\dot{\Phi} = \frac{d\Phi}{dt}$, $\alpha = \beta = 50$.

4 Simulation result of dynamic behavior of mechanism

The solution flowchart of dynamics of press mechanism considering dry friction clearances and

Fig. 4 Structural diagram of 2-DOF 9-bar press mechanism



lubricated clearances are depicted in Figs. 5 and 6, respectively.

As shown in Fig. 5, the specific steps are as follows.

- (1) Define simulation data and initial conditions of press mechanism.
- (2) The dry friction clearance model of the rotating pair is established and judge the collision state of the elements of the rotating pair. If the shaft and bearing do not collide, then $F_n = 0, F_t = 0$. If the shaft and bearing collide, the normal contact force F_n and tangential friction force F_t

are calculated according to L-N model and modified Coulomb friction model, respectively.

- (3) The dry friction clearance model is embedded into the rigid body dynamic equation established by Lagrange multiplier method, and its dynamics is solved based on fourth-order Runge–Kutta algorithm.
- (4) Cycle through the above steps until the simulation is complete.

As shown in Fig. 6, the specific steps are as follows.

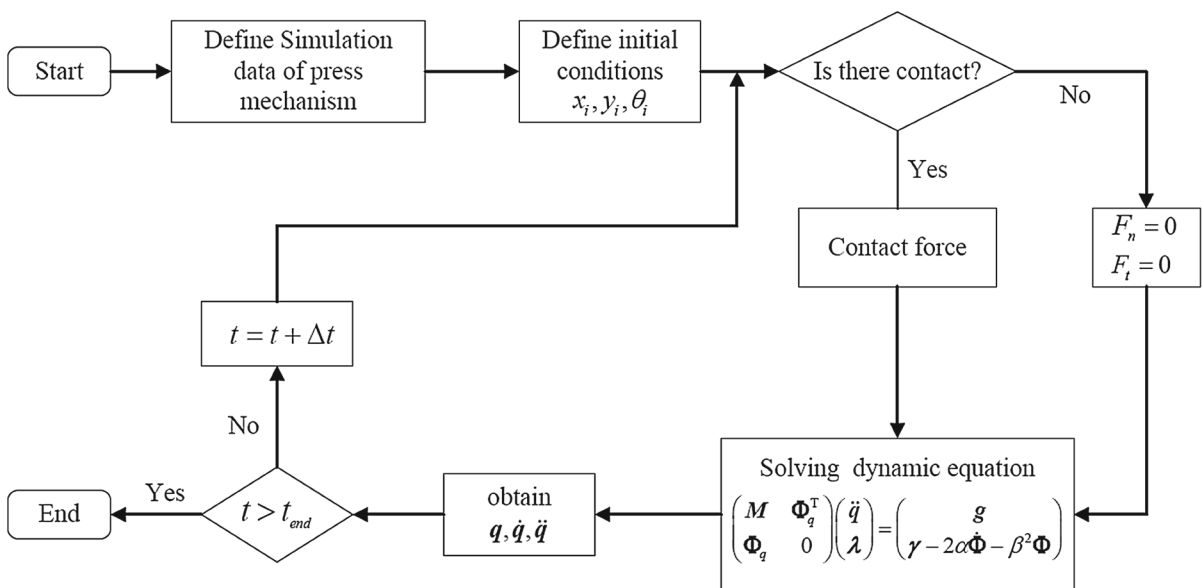


Fig. 5 The solution flowchart of dynamics of press mechanism considering dry friction clearances

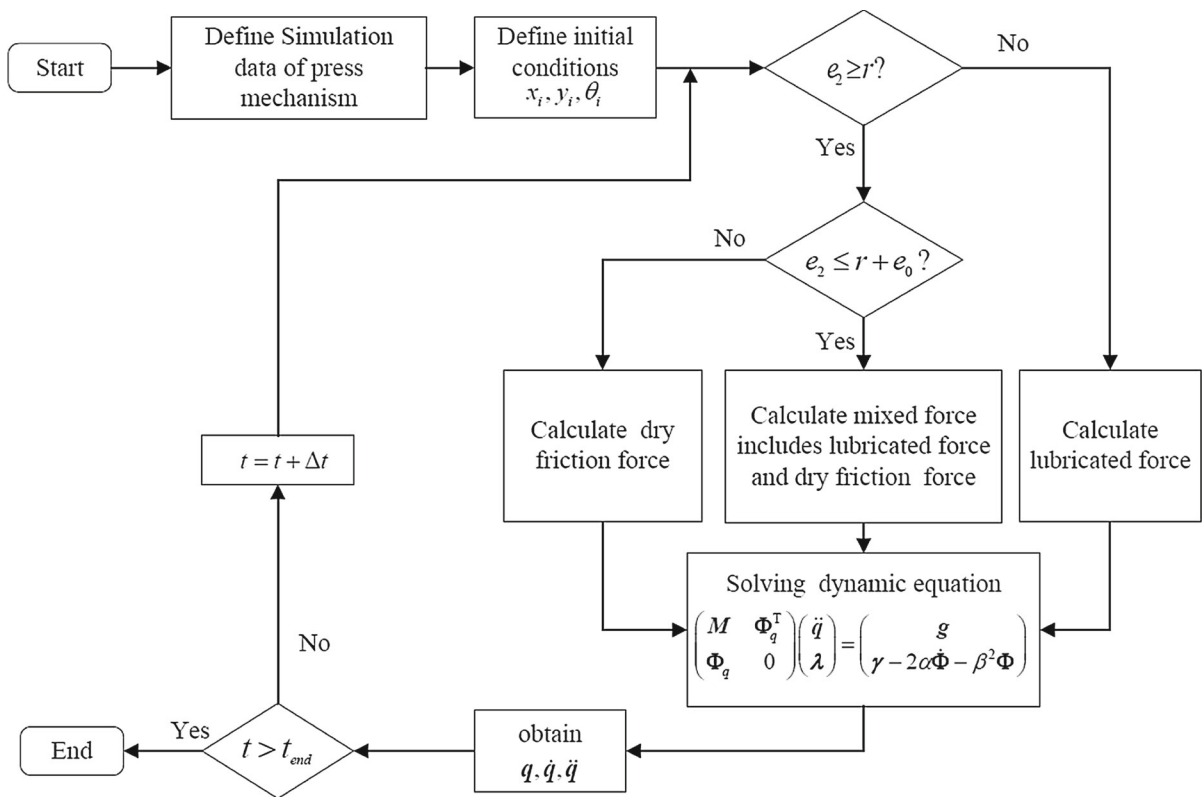


Fig. 6 The solution flowchart of dynamics of press mechanism considering lubricated clearances

- (1) Define simulation data and initial conditions of press mechanism.
- (2) The solution process of impact force of lubricated clearance is as follows. If $e_2 \leq r$, the shaft is not in direct contact with bearing, so only the lubricated force is considered. If $r \leq e_2 \leq r + e_0$, The shaft and bearing are in transition state, and mixed force includes lubricated force and dry friction force is considered. If $e_2 \geq r + e_0$, the shaft is in direct contact with bearing, so only the dry friction force is considered.
- (3) The lubricated clearance model is embedded into the rigid body dynamic equation established by Lagrange multiplier method, and its dynamics is solved based on fourth-order Runge–Kutta algorithm.
- (4) Cycle through the above steps until the simulation is complete.

Table 1 Simulation data of clearance

Parameter	Values	Parameter	Values
Bearing radius R_i	0.015(m)	limit speed v_1	0.001(m/s)
Bearing length L	0.04(m)	limit speed v_0	0.0001(m/s)
Dynamic viscosity μ	100cp	Elastic modulus of aluminum alloy	70(GPa)
Friction coefficient c_f	0.15	Elastic modulus of steel	206(GPa)
Integral step $d_r(s)$	0.0001	Exponent n	1.5
Recovery coefficient c_e	0.9	Modified interval e_0	2×10^{-6}
Poisson's ratio ν_b, ν_s	0.3		

Table 2 Simulation data of mechanism

Member	Mass (Kg)	Length (m)	Moment of inertia(Kg · m ²)
L_1	0.142	0.080	3.030×10^{-4}
L_2	0.284	0.250	1.479×10^{-3}
L_3	0.396	0.350	4.042×10^{-3}
L_4	0.142	0.080	3.029×10^{-4}
L_6	0.204	0.180	3.683×10^{-3}
L_7	0.277	0.247	3.076×10^{-3}
L_8	0.341	0.300	2.558×10^{-3}
S_9	0.112	–	2.320×10^{-4}
h_x	–	0.500	–
h_y	–	0	–

4.1 Simulation data

The simulation data of 2-DOF 9-bar press mechanism are shown in Tables 1 and 2.

4.2 Influence of clearance values on dynamic behavior

In this section, the influence of clearance values on dynamic behavior of press mechanism is researched. Choose the material of clearance-shaft as aluminum alloy, and the driving speeds are $\omega_1 = 2\pi\text{rad/s}$ $\omega_4 = -2\pi\text{rad/s}$. The impact of different clearance values of 0.3 mm, 0.5 mm and 0.8 mm on dynamic behavior of mechanism considering dry friction clearances and lubricated clearances is discussed, respectively.

The dynamic behavior of different clearance values to mechanism considering dry friction clearances is shown in Figs. 7, 8.

As is seen from Fig. 7, when the clearance values of dry friction clearance are 0.3 mm, 0.5 mm and

0.8 mm, respectively, the maximum displacement errors of slider are -0.00277 m , -0.00314 m and -0.00371 m , respectively, the maximum velocity errors are -0.0232 m/s , -0.0276 m/s and -0.0334 m/s , respectively, and the maximum acceleration errors are 1.721 m/s^2 , 1.888 m/s^2 and 4.214 m/s^2 , respectively. To summarize, with the increase in clearance values, the motion characteristics of slider fluctuate more and more, and the errors also increase. This is because the larger the clearance values, the more uncertain motion state between the elements of revolute clearance joint, resulting in the increase in the errors of slider.

As shown in Fig. 8, the impact force at clearance will continue to increase with the increase in clearance values. When the dry friction clearance values are 0.3 mm, 0.5 mm and 0.8 mm, respectively, the maximum impact forces at clearance A are 159.3 N, 315.4 N and 159.3 N, respectively, and the maximum impact forces at clearance B are 79.1 N, 320.8 N and 430.8 N, respectively. The impact force fluctuates

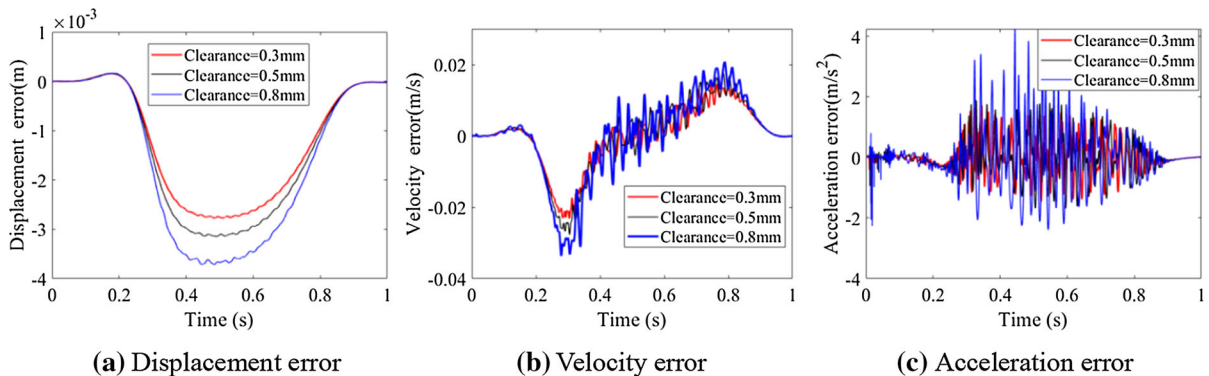
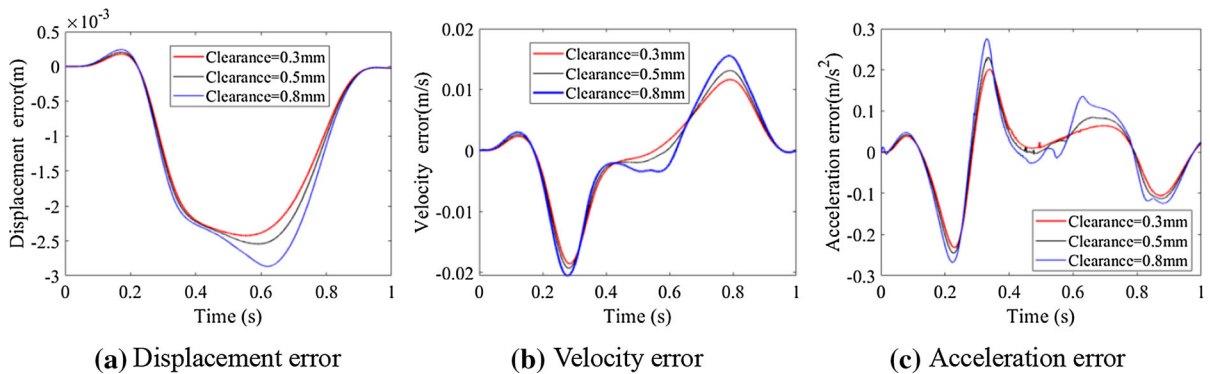
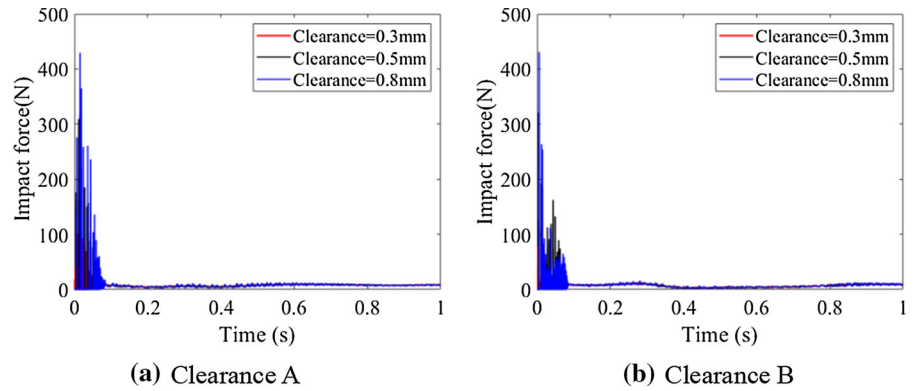
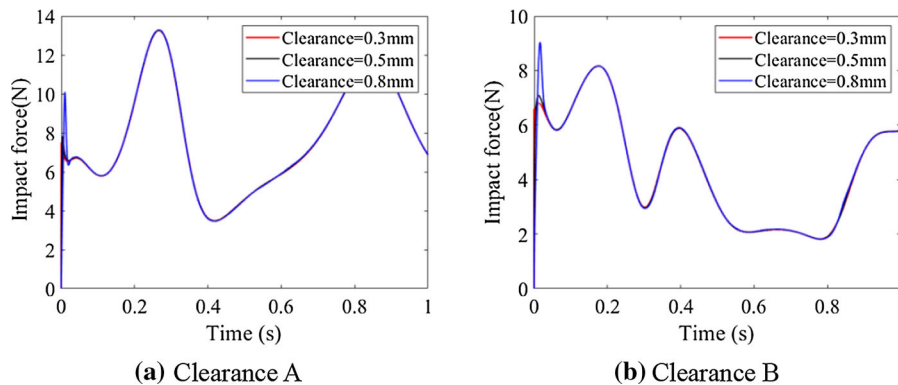


Fig. 7 The error of motion characteristics of slider

Fig. 8 Impact force of dry friction clearance**Fig. 9** The error of motion characteristics of slider**Fig. 10** Impact force of lubricated clearance

violently in the range of $[0, 0.08 \text{ s}]$ and tends to be flat after 0.08 s . This is because the shaft and bearing collide violently at the beginning of operation, so the impact force fluctuates greatly. After stable operation, the motion state of shaft and bearing is also relatively stable, so the impact force becomes stable.

The dynamic behavior of different clearance values to mechanism considering lubricated clearances is shown in Figs. 9, 10.

As can be seen from Fig. 9, when the clearance values of lubricated clearances are 0.3 mm , 0.5 mm and 0.8 mm , respectively, the maximum displacement errors of slider are 0.00242 m , 0.00254 m and 0.00286 m , respectively, the maximum velocity errors

are 0.0116 m/s, 0.0130 m/s and 0.0155 m/s, respectively, the maximum acceleration errors are 0.2012 m/s², 0.2304 m/s² and 0.2753 m/s², respectively. Consistent with the law of dry friction clearance, the errors of mechanism with lubricated clearances are also increasing when clearance values become larger. However, compared with the dry friction clearance, the lubricated clearances reduce the errors of the output response of mechanism, especially the acceleration error.

As shown in Fig. 10, the clearance value has little influence on impact force of lubricated clearance, and the impact force is only slightly different at the initial movement. Moreover, compared with the impact force considering dry friction clearance, the impact force considering lubricated clearance is greatly reduced. Therefore, lubricated clearance can reduce the influence of clearance effect on dynamic behavior of mechanism.

4.3 Influence of the material of clearance-shaft on dynamic behavior

Clearance-shaft of different materials have different elastic modulus, so in theory, the impact on mechanism with clearances during operation is different. In this section, the crank driving speeds are $\omega_1 = 3\pi\text{rad/s}$ $\omega_4 = 3\pi\text{rad/s}$ and the clearance values are 0.5 mm. The impact of clearance-shaft made of aluminum alloy and type 45 steel on dynamic behavior of press mechanism considering dry friction clearances and lubricated clearances are studied, respectively.

The dynamic behavior of different clearance-shaft to mechanism considering dry friction clearances is shown in Figs. 11, 12.

As shown in Figs. 11, 12, the different clearance-shaft materials have little impact on displacement and velocity of slider, but have an obvious influence on acceleration. When the material of clearance-shaft is aluminum alloy and type 45 steel, respectively, the maximum acceleration errors are 157.2 m/s² and 255.9 m/s², respectively; the maximum impact forces at clearance A are 319.4 N and 482.2 N, respectively, and the maximum impact forces at clearance B are 321.6 N and 540.7 N, respectively.

This result shows that the elastic modulus will have an impact on dynamic behavior of mechanism considering dry friction clearances, and the greater the elastic modulus of material, the greater the impact on dynamics of mechanism. This is because the greater the elastic modulus, the less easy the material is to deform and the stronger the brittleness, so the more violent vibration will be generated when the shaft collides with the bearing, resulting in the greater the collision force at the clearance.

The dynamic behavior of different clearance-shaft to mechanism considering lubricated clearances is shown in Figs. 13, 14.

As is seen from Figs. 13, 14, the different clearance-shaft materials have little influence on the motion characteristics and impact force of mechanism with lubricated clearances. According to the lubricated clearance model established in Sect. 2.2, the lubricating oil film will be formed between the shaft and bearing, so only the lubricated force is considered

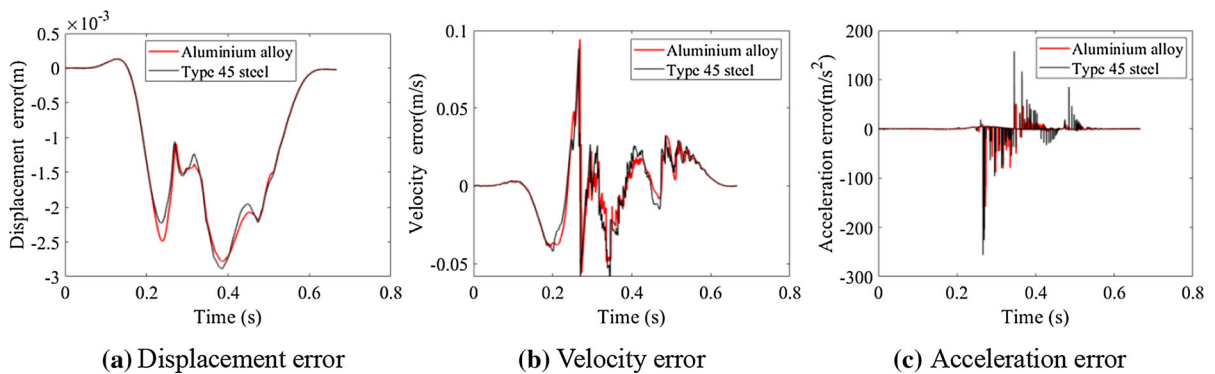
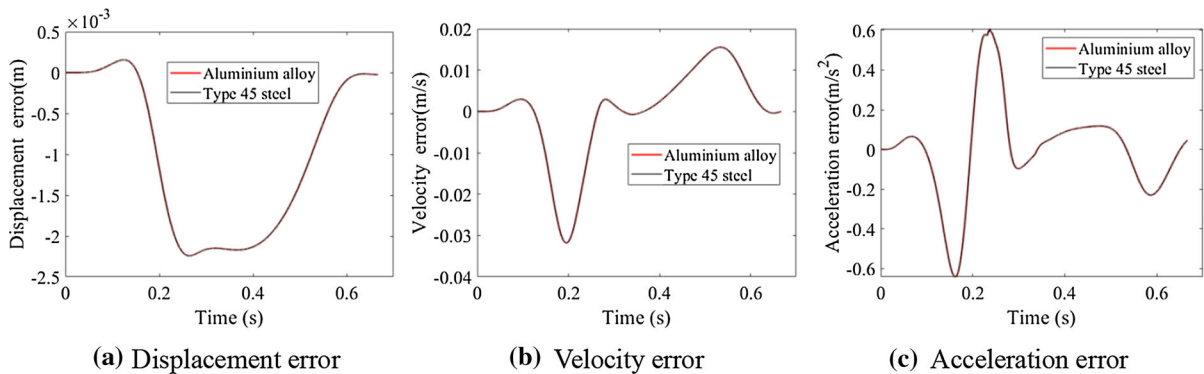
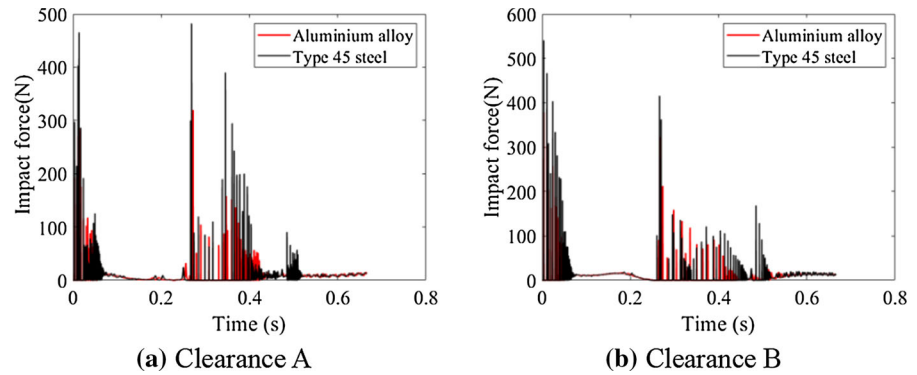
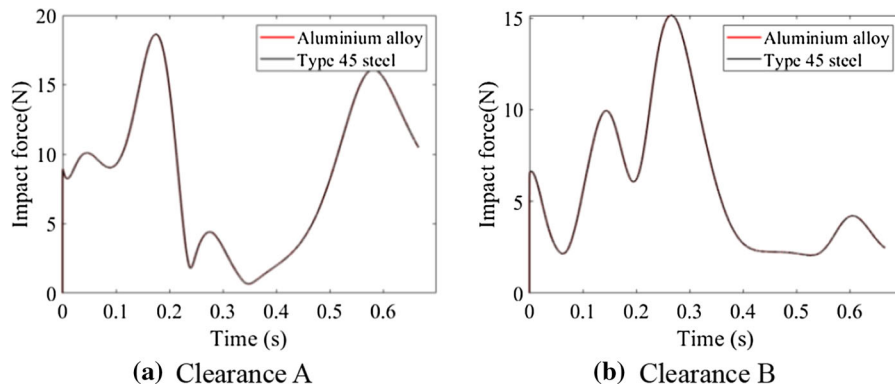


Fig. 11 The error of motion characteristics of slider

Fig. 12 Impact force of dry friction clearance**Fig. 13** The error of motion characteristics of slider**Fig. 14** Impact force of lubricated clearance

when $e_2 \leq r$. In other words, when the mechanism operates at medium or low speed, the shaft and bearing in the model will not be in direct contact due to the action of oil film. This is the reason that the material of clearance-shaft will hardly affect the mechanism with lubricated clearances.

4.4 Influence of crank driving speeds on dynamic behavior

In this section, the influence of different driving speeds on dynamic behavior of press mechanism considering dry friction clearances and lubricated clearances is

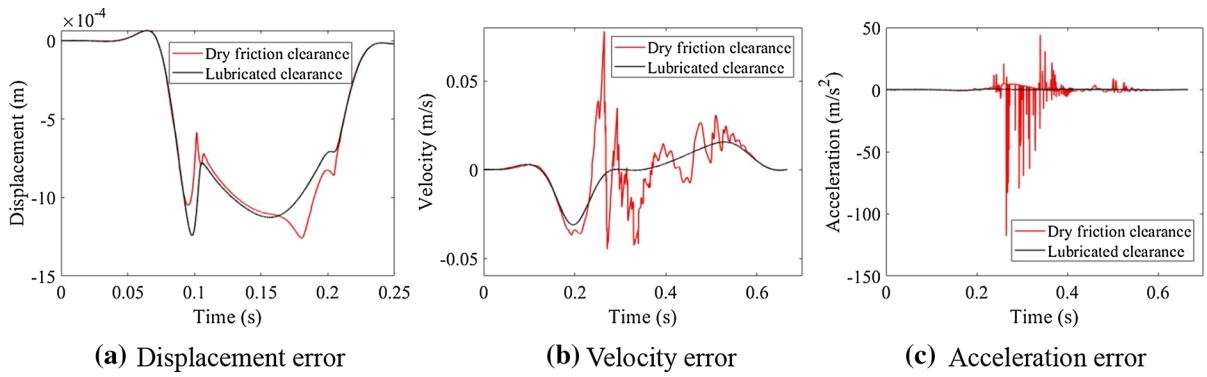


Fig. 15 The error of motion characteristics of slider when driving speeds are $\omega_1 = 3\pi\text{rad/s}$, $\omega_4 = -3\pi\text{rad/s}$

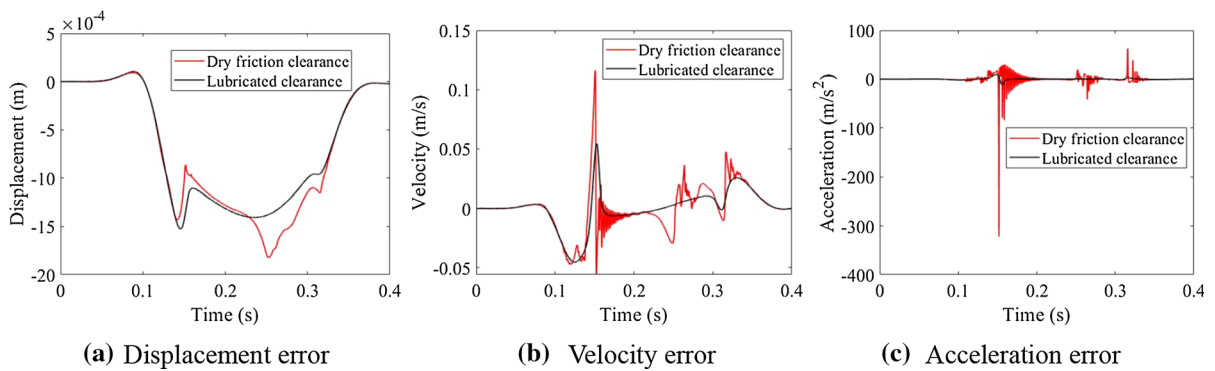


Fig. 16 The error of motion characteristics of slider when driving speeds are $\omega_1 = 5\pi\text{rad/s}$, $\omega_4 = -5\pi\text{rad/s}$

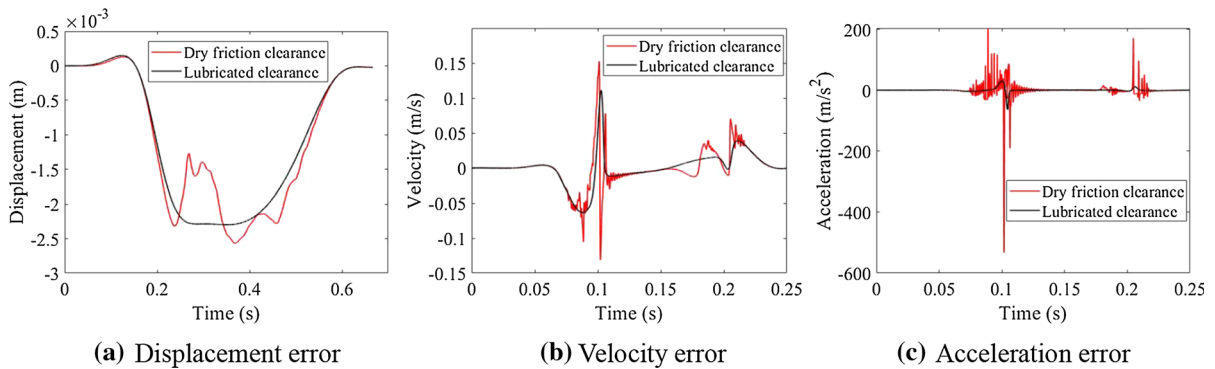


Fig. 17 The error of motion characteristics of slider when driving speeds are $\omega_1 = 8\pi\text{rad/s}$, $\omega_4 = -8\pi\text{rad/s}$

studied. The material of clearance-shaft is aluminum alloy, and the clearance value is 0.6 mm. The effects of driving speed on dynamic behavior of mechanism are discussed when driving speeds are $\omega_1 = 3\pi\text{rad/s}$, $\omega_4 = -3\pi\text{rad/s}$,

$\omega_1 = 5\pi\text{rad/s}$, $\omega_4 = -5\pi\text{rad/s}$ and $\omega_1 = 8\pi\text{rad/s}$, $\omega_4 = -8\pi\text{rad/s}$, respectively.

The influence of different driving speeds on dynamic behavior of mechanism with dry friction clearances and lubricated clearances is shown in Figs. 15, 17.

As is seen from Figs. 15, 16, 17, when dry friction clearances of press mechanism are considered, and when the driving speeds are $\omega_1 = 3\pi\text{rad/s}$, $\omega_4 = -3\pi\text{rad/s}$, $\omega_1 = 5\pi\text{rad/s}$, $\omega_4 = -5\pi\text{rad/s}$ and $\omega_1 = 8\pi\text{rad/s}$, $\omega_4 = -8\pi\text{rad/s}$, respectively, the maximum displacement errors of slider are 1.256×10^{-3} m, 1.819×10^{-3} m, 2.567×10^{-3} m, respectively, the maximum velocity error of slider are 0.0780 m/s, 0.1163 m/s, 0.1526 m/s, respectively, and the maximum acceleration error of slider are 117.8 m/s^2 , 317.4 m/s^2 , 533.2 m/s^2 , respectively. When lubricated clearances of mechanism are considered, and when the driving speeds are $\omega_1 = 3\pi\text{rad/s}$, $\omega_4 = -3\pi\text{rad/s}$, $\omega_1 = 5\pi\text{rad/s}$, $\omega_4 = -5\pi\text{rad/s}$ and $\omega_1 = 8\pi\text{rad/s}$, $\omega_4 = -8\pi\text{rad/s}$, respectively, the maximum displacement error of slider are 1.241×10^{-3} m, 1.525×10^{-3} m, 2.298×10^{-3} m, respectively, the maximum velocity error of

slider are 0.0310 m/s, 0.0545 m/s, 0.1109 m/s, respectively, and the maximum acceleration error of slider are 0.5652 m/s^2 , 11.69 m/s^2 , 64.38 m/s^2 , respectively. It can be seen that the displacement, velocity and acceleration errors of slider are increasing with the increase in the driving speeds. In addition, the lubricated clearances can reduce the output error of slider, especially the acceleration error.

The influence of different driving speeds on Impact force of clearance is shown in Figs. 18, 19, 20.

As is seen from Figs. 18, 19, 20, when dry friction clearances of press mechanism are considered, and when the driving speeds are $\omega_1 = 3\pi\text{rad/s}$, $\omega_4 = -3\pi\text{rad/s}$, $\omega_1 = 5\pi\text{rad/s}$, $\omega_4 = -5\pi\text{rad/s}$ and $\omega_1 = 8\pi\text{rad/s}$, $\omega_4 = -8\pi\text{rad/s}$, respectively, the maximum impact forces at clearance A are 233.3 N, 287.2 N and 753.1 N, respectively, and the maximum impact forces at clearance B are 322.6 N, 436.2 N and 926.4 N, respectively.

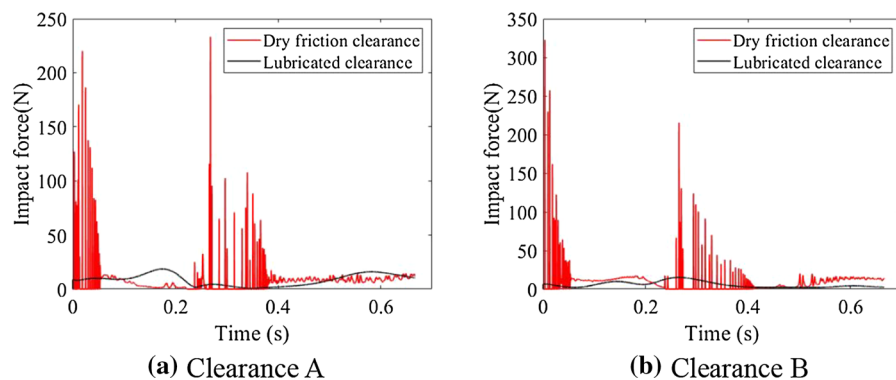


Fig. 18 Impact force of clearance when driving speeds are $\omega_1 = 3\pi\text{rad/s}$, $\omega_4 = -3\pi\text{rad/s}$

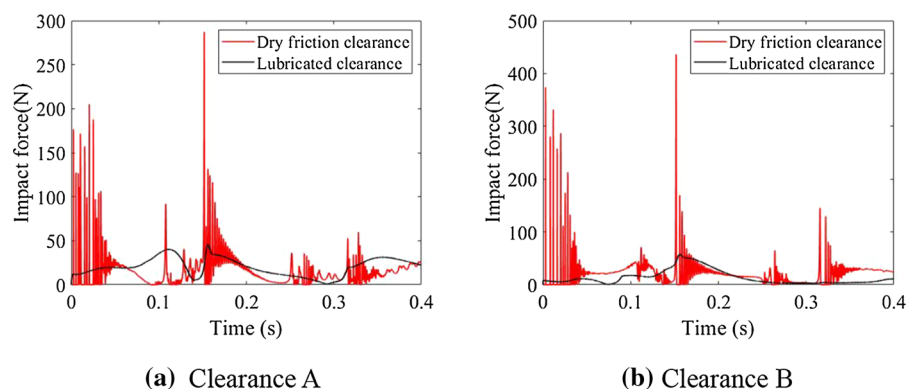


Fig. 19 Impact force of clearance when driving speeds are $\omega_1 = 5\pi\text{rad/s}$, $\omega_4 = -5\pi\text{rad/s}$

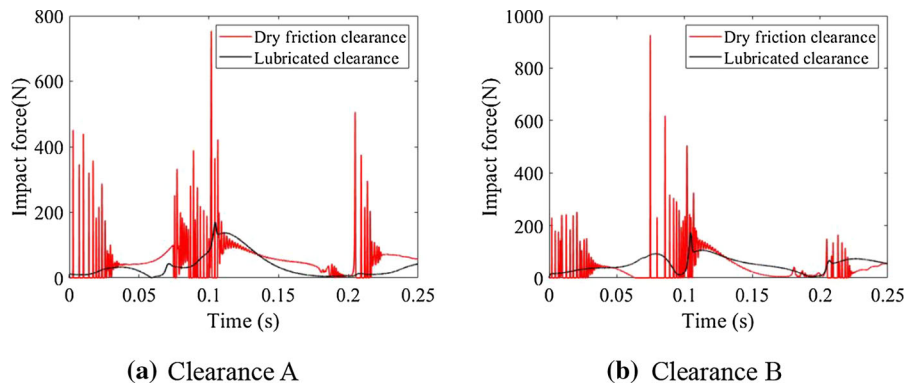
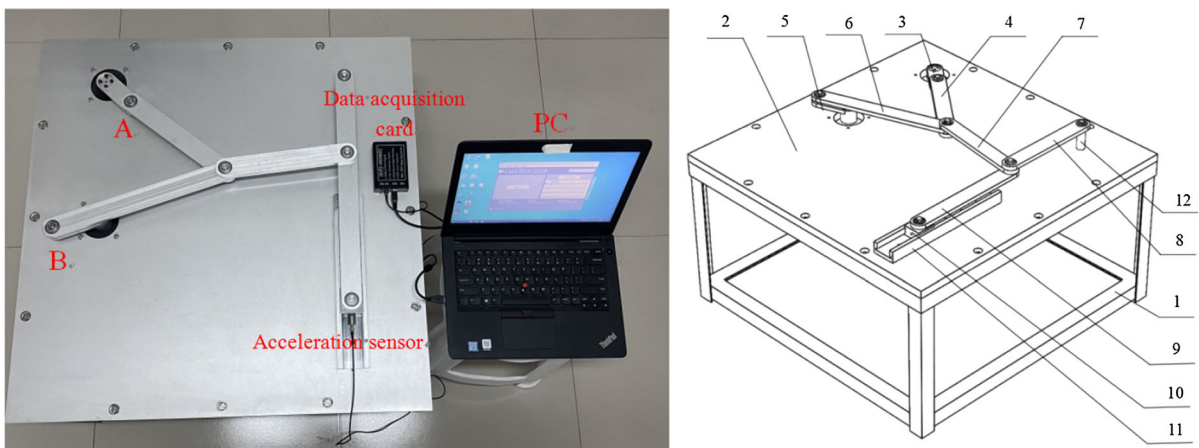


Fig. 20 Impact force of clearance when driving speeds are $\omega_1 = 8\pi\text{rad/s}$, $\omega_4 = -8\pi\text{rad/s}$



(a) Entity diagram

(b) Structure diagram

1-Frame, 2-Baseplate, 3-L₁, 4-L₂, 5-L₄, 6-L₃, 7-L₆, 8-L₇, 9-L₈, 10-Slider, 11-Guild rail, 12-Pin shaft

Fig. 21 Experimental platform of press mechanism

respectively. When lubricated clearances of press mechanism are considered, and when the driving speeds are $\omega_1 = 3\pi\text{rad/s}$, $\omega_4 = -3\pi\text{rad/s}$, $\omega_1 = 5\pi\text{rad/s}$, $\omega_4 = -5\pi\text{rad/s}$ and $\omega_1 = 8\pi\text{rad/s}$, $\omega_4 = -8\pi\text{rad/s}$, respectively, the maximum impact forces at clearance A are 18.61 N, 46.0 N and 170.5 N, respectively, and the maximum impact forces at clearance B are 15.18 N, 57.81 N and 174.2 N, respectively. In summary, with the continuous increase in the driving speed, the impact force of clearance increase accordingly. However, at the same driving speed, the peak impact force at the clearance of mechanism with lubricated clearance are much less than those with dry friction clearances. In addition, the

contact force at clearance B is greater than that at clearance A.

5 Experimental study

5.1 Construction of experimental platform

In this chapter, the simplified experimental platform of 2-DOF 9-bar press mechanism is built and the correctness of the theoretical results and the model is verified. This platform includes 2-DOF 9-bar mechanism, acceleration sensor, data acquisition card and PC terminal, as shown in Fig. 21. The material of the

experimental platform is aluminum alloy and the density is 2800 kg/m^3 .

The principle of the test is that the crank (L_1 and L_4) is driven to rotate by the servo motor, thereby driving the slider (S_9) to reciprocate in the guide rail. The end of slider is connected with an acceleration sensor (as shown in Fig. 22) to capture the acceleration signal of slider. The signal is collected by the data acquisition card (as shown in Fig. 23) and transmitted to the PC terminal, then the data are processed and stored by LabVIEW software.



Fig. 22 Type MPS-ACC01X acceleration sensor

Fig. 23 Type MPS-060602 data acquisition card



5.2 Experimental verification of the influence of clearance value on dynamic behavior

In this section, the influence of different clearance values on dynamic behavior of experimental platform is researched. Choose the driving speed as $\omega_1 = 3\pi \text{ rad/s}$ $\omega_4 = -3\pi \text{ rad/s}$, and the material of clearance-shaft is aluminum alloy. The effects of different clearance values on dynamic behavior of experimental platform with dry friction clearances and lubricated clearances are discussed, as shown in Figs. 24, 25. The experimental results and theoretical results are compared and analyzed, as shown in Figs. 26, 27.

As shown in Figs. 24, 25, the acceleration of slider in a period of time after the stable operation of mechanism is analyzed. The experimental results show that the acceleration trend of slider is completely consistent at different clearance values, and only the peak values is different. When clearance values are 0.3 mm and 0.6 mm, respectively, the maximum acceleration peaks of mechanism considering dry friction clearance are 52.78 m/s^2 and 64.41 m/s^2 , respectively. And the maximum acceleration peaks of mechanism considering lubricated clearances are 41.74 m/s^2 and 51.88 m/s^2 , respectively. It can be found that the acceleration of slider is larger when the clearance values is larger. And the lubricated clearances can reduce the peak values of acceleration of slider. This result also confirms the correctness of the theoretical analysis in Sect. 4.2.

As is seen from Figs. 26, 27, theoretical results and experimental results of different clearance values are compared when considering dry friction clearances and lubricated clearances of mechanism. The results

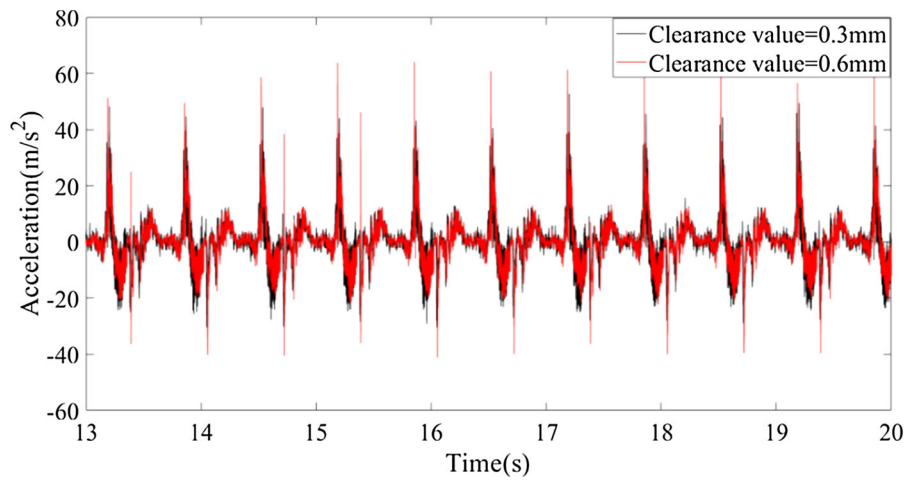


Fig. 24 Experimental study of different clearance values when considering dry friction clearance

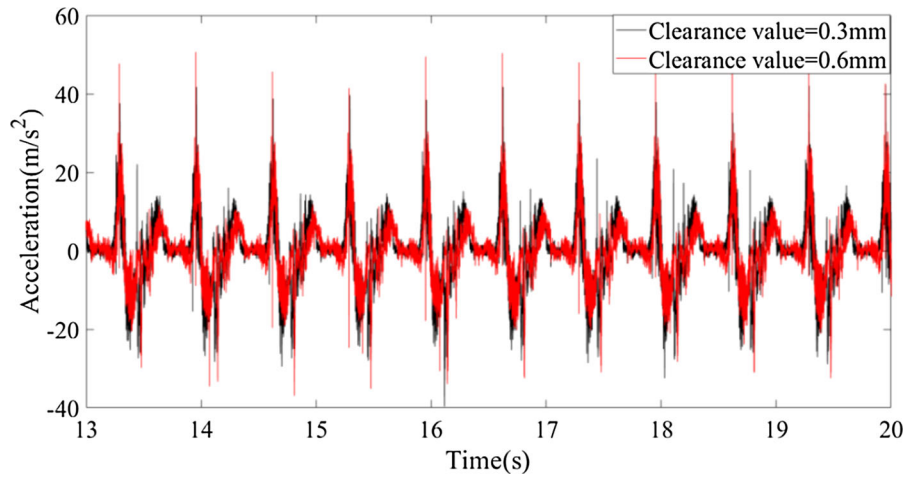


Fig. 25 Experimental study of different clearance values when considering lubricated clearance

Fig. 26 Comparison of acceleration of slider when considering dry friction clearance

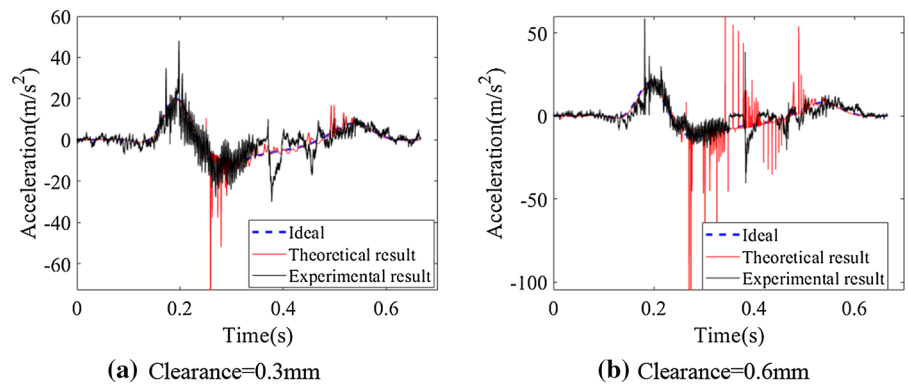


Fig. 27 Comparison of acceleration of slider when considering lubricated clearance

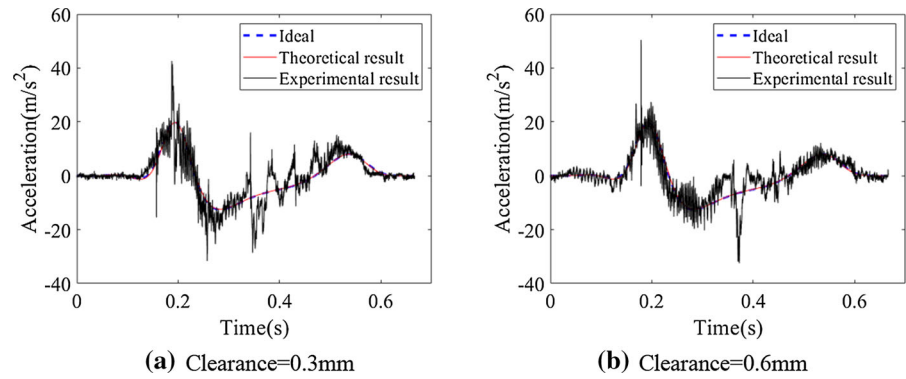


Fig. 28 Experimental study of different clearance values when considering dry friction clearance

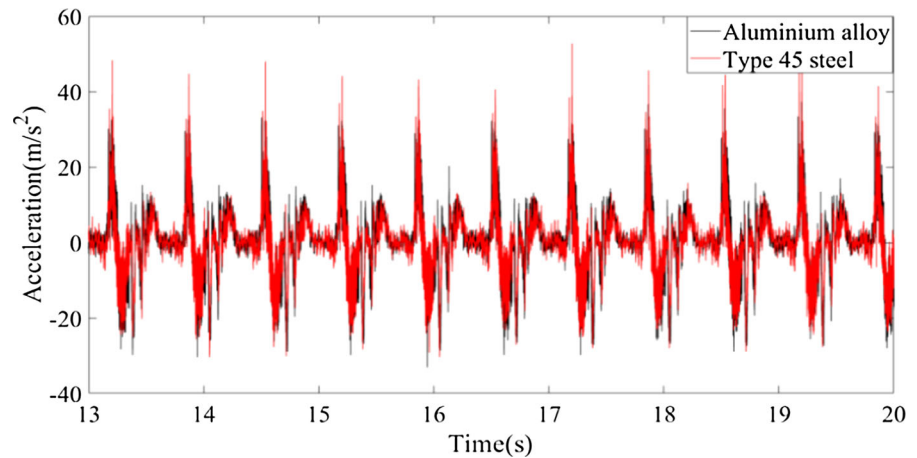
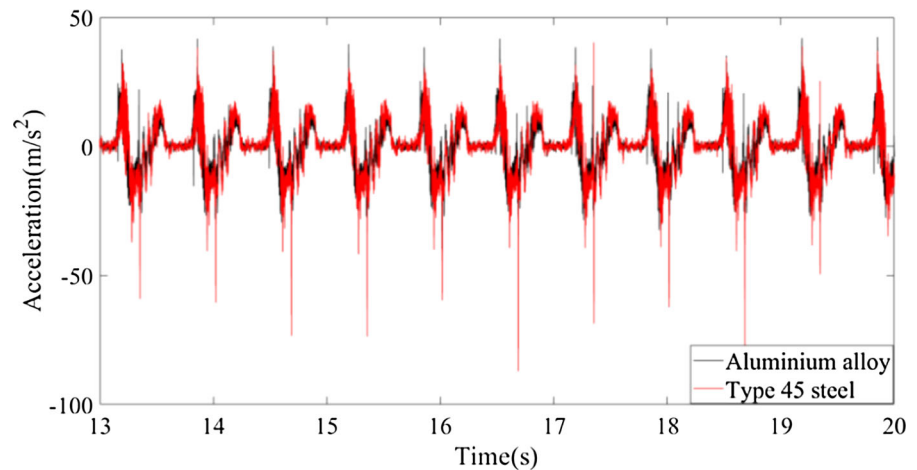


Fig. 29 Experimental study of different clearance values when considering lubricated clearance



show that the experimental results are basically consistent with the theoretical results. The peak value of theoretical result is larger than experimental result when considering dry friction clearances. The reason is that during the test, lubricant oil will be added

between the guide rail and the sliding block in order to make the mechanism run more smoothly, resulting in that the peak value of experimental acceleration of slider is smaller than theoretical acceleration.

Fig. 30 Comparison of acceleration of slider when considering dry friction clearance

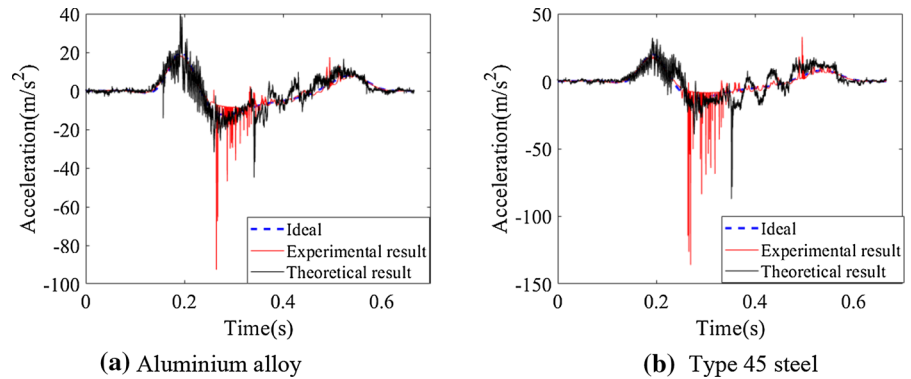
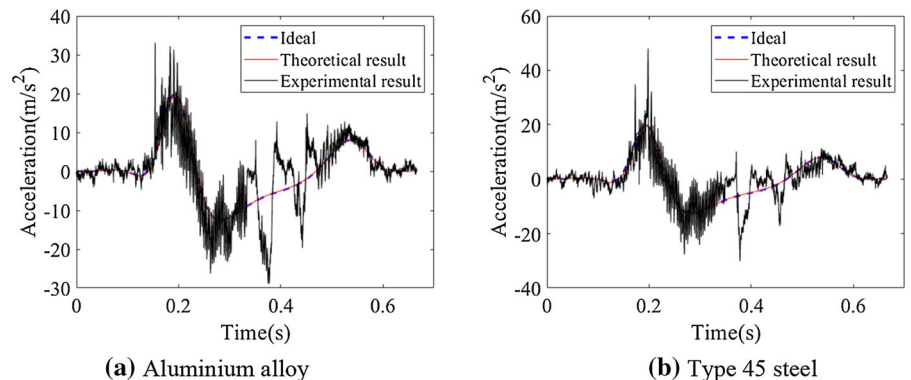


Fig. 31 Comparison of acceleration of slider when considering lubricated clearance



5.3 Experimental verification of the influence of material of clearance-shaft on dynamic behavior

In this section, the influence of different materials of clearance-shaft on dynamic behavior of experimental platform is researched. Choose the clearance values as 0.3 mm and the driving speeds are $\omega_1 = 3\pi\text{rad/s}$ $\omega_4 = -3\pi\text{rad/s}$. The material of clearance-shaft are aluminum alloy and type 45 steel, respectively. The impact of different clearance-shaft materials on dynamic behavior of experimental platform with dry friction clearances and lubricated clearances are discussed, as shown in Figs. 28, 29. The experimental results and theoretical results are compared and analyzed, as shown in Figs. 30, 31.

As is seen from Figs. 28, 29, when the material of clearance-shaft are aluminum alloy and type 45 steel, respectively, the maximum acceleration of mechanism considering dry friction clearance are 41.74 m/s^2 and 81.07 m/s^2 , respectively. And the maximum acceleration of mechanism considering lubricated clearance are 36.68 m/s^2 and 52.78 m/s^2 , respectively. It can be

found that the peak value of acceleration is greater when the material of clearance-shaft is type 45 steel. And compared to dry friction clearance, the lubricated clearances can reduce the peak acceleration of slider. This result proves the impact of the material of clearance-shaft on dynamic behavior of mechanism with dry friction clearance mentioned in Sect. 4.3. However, it is mentioned in Sect. 4.3 that the material of clearance-shaft has little impact on dynamic of mechanism with lubricated clearance, which is different from the results obtained in the experiment. This is because during the test, the extrusion force generated by the mechanism during dynamic operation is large, and the sealing performance of the sealing ring cannot be perfectly guaranteed, which leads to the inevitable leakage of lubricant oil. A more reliable sealing method will be considered in the later experimental study.

As shown in Figs. 30, 31, theoretical results and experimental results of different material of clearance-shaft are compared when considering dry friction clearances and lubricated clearances of mechanism. The results show that the experimental results are

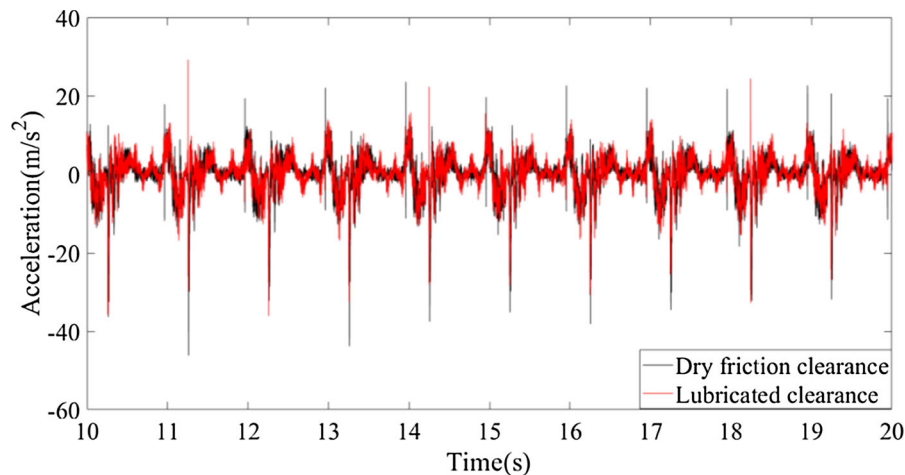


Fig. 32 Experimental study when driving speeds are $\omega_1 = 2\pi\text{rad/s}$ $\omega_4 = -2\pi\text{rad/s}$

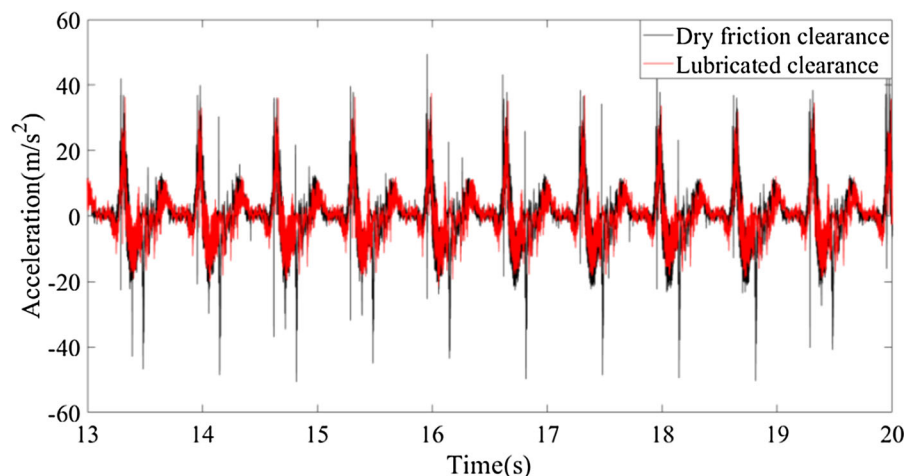


Fig. 33 Experimental study when driving speeds are $\omega_1 = 3\pi\text{rad/s}$ $\omega_4 = -3\pi\text{rad/s}$

basically consistent with the theoretical results, but the vibration frequency of the experimental results is higher. This is caused by vibration of experimental platform and accuracy errors of the measurement system.

5.4 Experimental verification of the influence of driving speeds on dynamic behavior

In this section, the influence of different driving speeds on dynamic behavior of experimental platform is researched. Choose the clearance value as 0.3 mm and the material of clearance-shaft is aluminum alloy. The dynamic behavior of experimental platform with dry friction clearances and lubricated clearances is

analyzed when driving speeds are $\omega_1 = 2\pi\text{rad/s}$ $\omega_4 = -2\pi\text{rad/s}$ and $\omega_1 = 3\pi\text{rad/s}$ $\omega_4 = -3\pi\text{rad/s}$, as shown in Figs. 32, 33. The experimental results and theoretical results are compared and analyzed, as shown in Figs. 34, 35.

As shown in Fig. 32, when the driving speeds are $\omega_1 = 2\pi\text{rad/s}$ $\omega_4 = -2\pi\text{rad/s}$, the maximum acceleration of mechanism considering dry friction clearance and lubricated clearance are 46.22 m/s^2 and 36.08 m/s^2 , respectively. As shown in Fig. 33, when the driving speeds are $\omega_1 = 3\pi\text{rad/s}$ $\omega_4 = -3\pi\text{rad/s}$, the maximum acceleration of mechanism considering dry friction clearances and lubricated clearances are 56.37 m/s^2 and 37.57 m/s^2 , respectively. The existence of lubricated clearance reduces

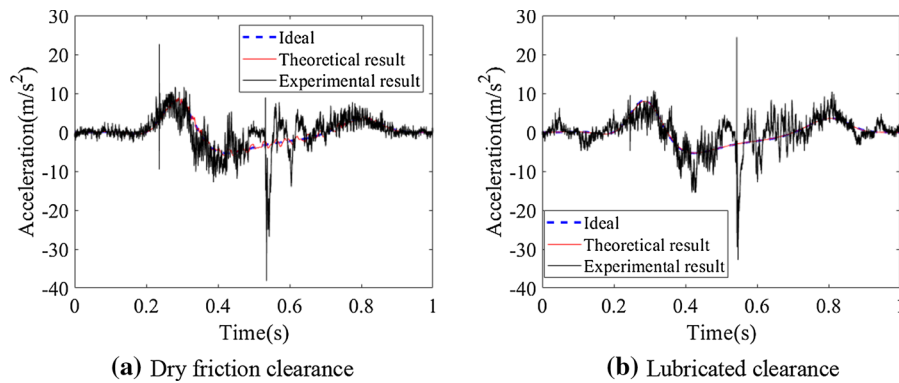


Fig. 34 Comparison of acceleration of slider when driving speeds are $\omega_1 = 2\pi\text{rad/s}$, $\omega_4 = -2\pi\text{rad/s}$

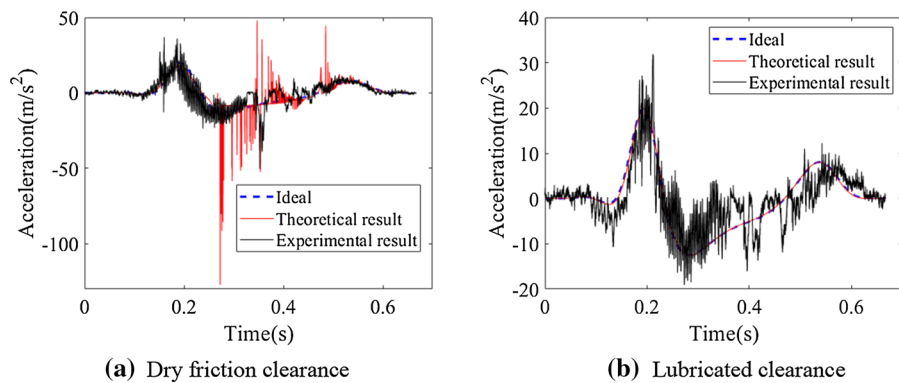


Fig. 35 Comparison of acceleration of slider when driving speeds are $\omega_1 = 3\pi\text{rad/s}$, $\omega_4 = -3\pi\text{rad/s}$

the acceleration of slider, which is consistent with the conclusion in Sect. 4.4. In addition, the higher the driving speed, the greater the peak acceleration of mechanism, which is consistent with the results of theoretical analysis.

As shown in Figs. 34, 35, the acceleration of mechanism considering dry friction clearances and lubricated clearances is compared with the theoretical results, respectively. And the results show that the trend of the experimental result is basically consistent with the theoretical results.

6 Conclusions

Experimental verification of dynamic behavior for multi-link press mechanism with 2D revolute joint considering dry friction clearances and lubricated clearances is researched in this paper, main conclusions are as follows:

- (1) The dry friction clearance model and lubricated clearance model are established and the rigid body dynamic model of press mechanism considering 2D revolute clearances based on Lagrange multiplier method is developed.
- (2) The impact of clearance values, material of clearance-shaft and driving speeds on dynamic behavior of mechanism with dry friction clearances and lubricated clearances are researched. The results show that the larger the clearance values and driving speeds, the larger the output errors and impact force of mechanism. The material of clearance-shaft has a great influence on mechanism considering dry friction clearances, but has little influence on mechanism considering lubricated clearances.
- (3) The experimental platform of 2-DOF 9-bar press mechanism with clearances is built, and the effects of different factors on its dynamic behavior are studied. The results show that the trend of the theoretical results is basically

consistent with the test results under different parameters, so thus to verify the correctness of theoretical model and analysis.

Acknowledgments This research is supported by Shandong key research and development public welfare program (2019GGX104011), Natural Science Foundation of Shandong Province (GrantNo.ZR2017MEE066).

Conflict of interest The authors declare that they have no conflict of interest.

Ethical approval This manuscript has not been published, simultaneously submitted or already accepted for publication elsewhere. All authors have read and approved the manuscript. There is no conflict of interest related to individual authors' commitments and any project support. All acknowledged persons have read and given permission to be named. Xiulong CHEN has nothing to disclose.

Data availability The data used to support the findings of this study are included within the article.

References

- Li, X., Ding, X., Chirikjian, G.S.: Analysis of angular-error uncertainty in planar multiple-loop structures with joint clearances[J]. *Mech. Mach. Theory* **91**, 69–85 (2015)
- Erkaya, S.: Effects of joint clearance on the motion accuracy of robotic manipulators[J]. *J. Mech. Eng.* **64**(2), 82–94 (2018)
- Erkaya, S., Doğan, S., Şefkathioğlu, E.: Analysis of the joint clearance effects on a compliant spatial mechanism[J]. *Mech. Mach. Theory* **104**, 255–273 (2016)
- Pei, J., Han, X., Tao, Y., et al.: Lubrication reliability analysis of spur gear systems based on random dynamics[J]. *Tribol. Int.* **153**, 106606 (2020)
- Raymand, G.A., Amalraj, I.J.: Inertia effects in rheodynamic lubrication of an externally pressurized converging thrust bearing using Herschel-Bulkley fluids[J]. *J. Appl. Fluid Mech.* **13**(4), 1245–1252 (2020)
- Fang, C., Meng, X., Lu, Z., et al.: Modeling a lubricated full-floating pin bearing in planar multibody systems[J]. *Tribol. Int.* **131**, 222–237 (2019)
- Reis, V.L., Daniel, G.B., Cavalca, K.L.: Dynamic analysis of a lubricated planar slider-crank mechanism considering friction and Hertz contact effects[J]. *Mech. Mach. Theory* **74**, 257–273 (2014)
- Abdallah, M.B., Khemili, I., Aifaoui, N.: Numerical investigation of a flexible slider-crank mechanism with multijoints with clearance[J]. *Multibody Sys.Dyn.* **38**(2), 173–199 (2016)
- Miao, H., Li, B., Liu, J., et al.: Effects of revolute clearance joint on the dynamic behavior of a planar space arm system[J]. *Proc. Inst. Mech. Eng.* **233**(5), 1629–1644 (2019)
- Marques, F., Isaac, F., Dourado, N., et al.: A Study on the dynamics of spatial mechanisms with frictional spherical clearance joints[J]. *J. Comput. Nonlinear Dyn.* **12**(5), 051013 (2017)
- Chen, X., Wang, T., Jiang, S.: Study on dynamic behavior of planar multibody system with multiple lubrication clearance joints[J]. *Eur. J. Mech. A/Solids* (2022). <https://doi.org/10.1016/j.euromechsol.2021.104404>
- Geng, X., Wang, X., Wang, L., et al.: Non-probabilistic time-dependent kinematic reliability assessment for function generation mechanisms with joint clearances[J]. *Mech. Mach. Theory* **104**, 202–221 (2016)
- Jiang, S., Chen, X.: Reducing undesirable effects of clearances on dynamic and wear of planar multi-link mechanism[J]. *Nonlinear Dyn.* **100**(2), 1173–1201 (2020)
- Brogliato, B.: Feedback control of multibody systems with joint clearance and dynamic backlash: a tutorial[J]. *Multibody Sys.Dyn.* **42**(3), 283–315 (2017)
- Pandey, M.D., Zhang, X.: System reliability analysis of the robotic manipulator with random joint clearances[J]. *Mech. Mach. Theory* **58**, 137–152 (2012)
- Xiang, W., Yan, S., Wu, J.: Dynamic analysis of planar mechanical systems considering stick-slip and Stribeck effect in revolute clearance joints[J]. *Nonlinear Dyn.* **95**(1), 321–341 (2019)
- Singh, A., Sharma, S.C.: Analysis of a double layer porous hybrid journal bearing considering the combined influence of wear and non-Newtonian behaviour of lubricant[J]. *Meccanica* **56**(1), 73–98 (2021)
- Bai, Z., Zhao, J.: A study on dynamic characteristics of satellite antenna system considering 3D revolute clearance joint[J]. *Int. J. Aerosp. Eng.* **2020**, 8846177 (2020)
- Erkaya, S., Uzmay, I.: Experimental investigation of joint clearance effects on the dynamics of a slider-crank mechanism[J]. *Multibody Sys.Dyn.* **24**(1), 81–102 (2010)
- Flores, P., Koshy, C.S., Lankarani, H.M., et al.: Numerical and experimental investigation on multibody systems with revolute clearance joints[J]. *Nonlinear Dyn.* **65**(4), 383–398 (2011)
- Erkaya, S., Dogan, S., Ulus, S.: Effects of joint clearance on the dynamics of a partly compliant mechanism: numerical and experimental studies[J]. *Mech. Mach. Theory* **88**, 125–140 (2015)
- Akhadkar, N., Acary, V., Brogliato, B.: Multibody systems with 3D revolute joints with clearances: an industrial case study with an experimental validation[J]. *Multibody Sys.-Dyn.* **42**(3), 249–282 (2018)
- Qian, M., Qin, Z., Yan, S., et al.: A comprehensive method for the contact detection of a translational clearance joint and dynamic response after its application in a crank-slider mechanism[J]. *Mech. Mach. Theory* **145**, 103717 (2020)
- Cavaliere, F.J., Cardona, A.: Non-smooth model of a frictionless and dry three-dimensional revolute joint with clearance for multibody system dynamics[J]. *Mech. Mach. Theory* **121**, 335–354 (2018)
- Wu, X., Sun, Y., Wang, Y., et al.: Dynamic analysis of the double crank mechanism with a 3D translational clearance joint employing a variable stiffness contact force model[J]. *Nonlinear Dyn.* **99**(3), 1937–1958 (2020)
- Tan, X., Chen, G., Shao, H.: Modeling and analysis of spatial flexible mechanical systems with a spherical clearance joint based on the luGre friction model[J]. *J. Comput. Nonlinear Dyn.* **15**(1), 011005 (2019)

27. Ahmedalbashir, M., Romdhane, L., Lee, J.: Dynamics of a four-bar mechanism with clearance and Springs-Modeling and experimental analysis[J]. *J. Mech. Sci. Technol.* **31**(3), 1023–1033 (2017)
28. Wang, G., Qi, Z., Jing, W.: A differential approach for modeling revolute clearance joints in planar rigid multibody systems[J]. *Multibody Sys.Dyn.* **39**(4), 311–335 (2017)
29. Guo, J., Randall, R.B., Borghesani, P., et al.: A study on the effects of piston secondary motion in conjunction with clearance joints[J]. *Mech. Mach. Theory* **149**, 103824 (2020)
30. Amiri, A., Dardel, M., Daniali, H.M.: Effects of passive vibration absorbers on the mechanisms having clearance joints[J]. *Multibody Sys.Dyn.* **47**(4), 363–395 (2019)
31. Ordiz, M., Cuadrado, J., Cabello, M., et al.: Prediction of fatigue life in multibody systems considering the increase of dynamic loads due to wear in clearances[J]. *Mech. Mach. Theory* **160**(5), 104293 (2021)
32. Farahan, S.B., Ghazavi, M.R., Rahmanian, S.: Bifurcation in a planar four-bar mechanism with revolute clearance joint[J]. *Nonlinear Dyn.* **87**(2), 955–973 (2017)
33. Zheng, X., Zhang, R., Wang, Q.: Comparison and analysis of two Coulomb friction models on the dynamic behavior of slider-crank mechanism with a revolute clearance joint[J]. *Appl. Math. Mech.* **39**(9), 1239–1258 (2018)
34. Li, J., Huang, H., Yan, S., et al.: Kinematic accuracy and dynamic performance of a simple planar space deployable mechanism with joint clearance considering parameter uncertainty[J]. *Acta Astronaut.* **136**, 34–45 (2017)
35. Zheng, X., Fei, Z., Qi, W.: Modeling and simulation of planar multibody systems with revolute clearance joints considering stiction based on an LCP method[J]. *Mech. Mach. Theory* **130**, 184–202 (2018)
36. Soong, K., Thompson, B.S.: A theoretical and experimental investigation of the dynamic response of a slide-crank mechanism with radial clearance of the gudgeon-pin joint[J]. *J. Mech. Des.* **112**(2), 183–189 (1990)
37. Flores, P., Ambrósio, J., Claro, J., et al.: Lubricated revolute joints in rigid multibody systems[J]. *Nonlinear Dyn.* **56**(3), 277–295 (2009)

Publisher's Note Springer Nature remains neutral with regard to jurisdictional claims in published maps and institutional affiliations.